

Synthesis, characterization and curing behavior of methyl-tri(phenylethynyl)silane

Dexin Tan¹ · Xiaole Wu¹ · Yanli Wang² ·
Yuan Xu¹ · Honglong Xing¹

Received: 5 July 2015 / Accepted: 28 September 2015 / Published online: 15 October 2015
© Springer Science+Business Media Dordrecht 2015

Abstract Methyl-tri(phenylethynyl)silane ((ph-C≡C)₃-Si-CH₃) (MTPES) was synthesized with methyltrichlorosilane and phenylethyne by Grignard reaction. Its molecular structure was characterized by Fourier transform infrared spectroscopy, nuclear magnetic resonance (¹H-NMR, ¹³C-NMR, and ²⁹Si-NMR). Its curing behavior was analyzed by non-isothermal differential scanning calorimetry and rheometry, and the corresponding kinetic parameters and kinetic model were also discussed by Kissinger, Ozawa, Flynn–Wall–Ozawa and Friedman methods. The results showed that the melting point of MTPES was 130 °C and the processing window was 200 °C. The activation energy E_a , pre-exponential factor $\ln A$ and the reaction order n , m were 112.58 kJ/mol, 21.22 (s⁻¹), 1.20 and 0.56, respectively. The curing behavior of MTPES followed the autocatalytic kinetic model.

Keywords Methyl-tri(phenylethynyl)silane · Grignard reaction · Curing behavior · Differential scanning calorimetry · Rheometry

Introduction

The silicon-containing arylacetylenic monomer has received intense interest. This kind of arylacetylenic monomer can cure to form a crosslinked structure by thermal self-polymerization with the advantage of a large processing window [1, 2]. In addition, its polymers have the properties of high temperature resistance, high char yield and high radiation resistance. All these properties support potential

✉ Dexin Tan
tdxin@163.com

¹ School of Chemical Engineering, Anhui University of Science and Technology, Huainan 232001, China

² School of Materials Science and Engineering, Anhui University of Science and Technology, Huainan 232001, China

applications in biomaterials, optoelectronics, wave-transmitting materials, semiconductor materials, ceramic precursors and so forth [3, 4].

Numerous examples with different substituents at the Si bond, such as hydrogen, alkyl, phenyl or vinyl groups, have been reported [5–9]. Wrackmeyer et al. [8] divided the preparation of various alkynylsilanes into two methods. One is that of sophisticated reactions with rigorous reaction conditions and expensive raw materials (e.g. ruthenium), which are mainly limited to laboratory preparation. The other is that of conventional reactions of commercial chlorosilanes with alkynyllithium or ethynyl magnesium reagents. In these cases, Grignard reactions are mild, and some silicon-containing arylacetylenic monomers (e.g., methyl-di(phenylethynyl)silane) are also prepared by Grignard reactions and the yields are better than 75 % [10, 11].

As a kind of silicon-containing arylacetylene monomer, methyl-tri(phenylethynyl)silane (MTPES) was first reported using dianionic hexacoordinated silicon complexes, sodium bis(benzene-1,2-diolato) methylsilicate and phenylacetylene as raw materials by Grignard reagent or organolithium reagents, and the effects of different organometallic reagents, reaction time and temperature on yield were discussed [12, 13]. Kim and Wrackmeyer prepared the MTPES with phenylacetylene and lithium reagent, and made a basic structural analysis by nuclear magnetic resonance (NMR) and X-ray diffraction (XRD) [8, 14]. Zhou et al. also synthesized the MTPES with butyllithium and phenylacetylene and further confirmed its molecule structure by high resolution mass spectrometer (HRMS), Fourier transform infrared spectroscopy (FT-IR), NMR and elemental analysis (EA). At the same time, the reaction activation energy and reaction order were also obtained using Kissinger and Ozawa methods by differential scanning calorimetry (DSC) curves [15, 16]. However, the synthetic route with methyltrichlorosilane and phenylethylene, and the corresponding curing process (curing schedule, curing kinetic model) are not reported.

In this study, we prepared MTPES using the relative inexpensive methyltrichlorosilane and phenylethylene by Grignard reaction and the corresponding curing schedule was obtained by DSC and was further verified by FT-IR and rheometry. The kinetic parameters were obtained combined with Kissinger, Ozawa, Flynn–Wall–Ozawa and Friedman methods, and the kinetic model was also established.

Experimental

Materials and methods

Phenylacetylene and methyltrichlorosilane was obtained from aike Reagent Company, China. Magnesium ribbons (Chengdu KeLong Chemical Company) were treated before being used. All chemicals and solvents were used according to standard treatment procedures.

Preparation of methyl-tri(phenylethynyl)silane monomer

At first, magnesium Grignard reagent was prepared as follows: The magnesium metal ribbon (1.68 g) was introduced into a 125-ml, three-necked round bottom

flask with a condenser, a dropping funnel, nitrogen gas and a stirrer. THF (20 ml) was introduced into the flask, a small piece of iodine was added and then the mixture was stirred to activate the reaction. A solution of 5 ml ethylbromide in THF (25 ml) was added dropwise to the activated magnesium at room temperature over the course of about 1 h. The resulting mixture continued to be refluxed over 3 h to produce ethylmagnesium bromide.

Then a solution of 7.4 ml phenylacetylene in THF (25 ml) was added dropwise in an ice-bath over the course of 1 h, and the reaction was secondly refluxed over 3 h to prepare the phenylethynylene Grignard reagent. The MTPES was prepared by the following procedures: 2.6 ml methyl-trichlorosilane in THF (25 ml) was added dropwise to the flask in an ice-bath over 1 h and refluxed over 3 h. The solution was gradually added as 33 ml of 1 mol/l aqueous solution of hydrochloric acid after cooling. Toluene (12.5 ml) was used to separate the oil phase, which was then washed with distilled water until neutral, followed by drying to stand overnight. The solvent was distilled off with vacuum distillation to eventually give an orange crude product, and was further recrystallized in ethanol to cause repeated precipitation. The precipitates were filtered off and branch shape crystals were obtained (5.08 g, 65.76 % yield) (Fig. 1a).

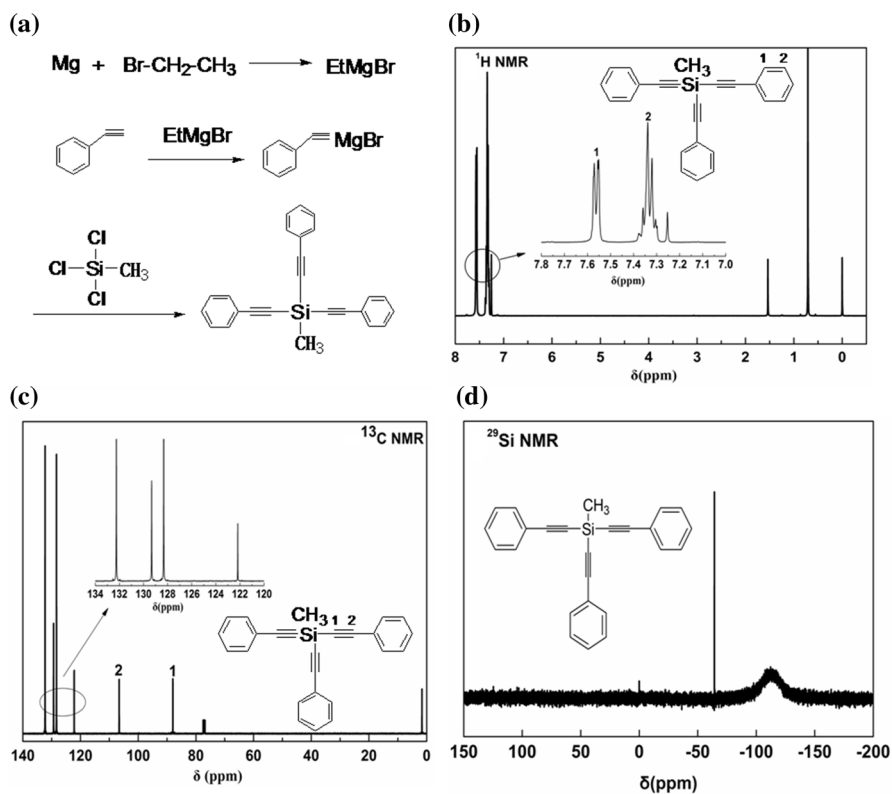


Fig. 1 Synthesis and structural information of MTPES (a synthetic route, b $^1\text{H-NMR}$, c $^{13}\text{C-NMR}$, d $^{29}\text{Si-NMR}$)

Characterization

FT-IR spectrum was carried out with Nicolet 380 FT-IR Spectrometer by potassium bromide (KBr) pellets. $^1\text{H-NMR}$, $^{13}\text{C-NMR}$ and $^{29}\text{Si-NMR}$ spectra were traced on an AVANCE AV-400 Super-conducting Fourier Digital NMR Spectrometer (400 MHz for $^1\text{H-NMR}$, 100.61 MHz for $^{13}\text{C-NMR}$ and 79.49 MHz for $^{29}\text{Si-NMR}$). The chemical shifts were recorded relative to tetramethylsilane (δ , 0.0 ppm) for $^1\text{H-NMR}$, $^{29}\text{Si-NMR}$ and CDCl_3 (δ , 77.7 ppm) for $^{13}\text{C-NMR}$. The DSC was operated on a NETZSCH STA 449F3 instrument at the flow rate of 20 m/min nitrogen atmosphere. Rheological behavior was traced by TA AR-G2 Rheometer at 3 °C/min and a shear rate of 0.01 s^{-1} .

Results and discussion

Structural analysis of MTPES

$^1\text{H-NMR}$ spectrum of MTPES is shown in Fig. 1b. The silicon methyl protons resonates at 0.71 ppm and aromatic hydrogen resonates at 7.32–7.56. In a precise NMR peak integration, the ratio of methyl protons (m, 3H, CH_3 –), aromatic hydrogen (m, 6H, $\text{PhH-C}\equiv\text{C}$) adjacent to ethynyl and other aromatic hydrogens (m, 9H, PhH) is 3:6:9.

The carbon spectrum of MTPES is described in Fig. 1c. The methyl bonded to the silicon was 1.63 ppm (Si-CH_3). The acetylenic carbons appear at 88 and 106 ppm, bonded to the silicon and phenyl unit. The phenyl carbons are symmetrical and have resonances between 122.17 and 132.53 ppm. $^{29}\text{Si-NMR}$ spectrum of MTPES is presented in Fig. 1d. The signal peak assigned to the silicon is observed at -64.22 ppm, while the road peak at about -110 ppm may be caused by the silicon dioxide in the NMR tube. Based on the $^1\text{H-NMR}$, $^{13}\text{C-NMR}$, $^{29}\text{Si-NMR}$ spectra, the results are in agreement with the structure of MTPES [8, 15].

Curing behavior of MTPES

Curing schedule of MTPES

Figure 2 shows the DSC thermograms of MTPES at different heating rates. The endothermal peak at 130 °C is the melting point, and the initial curing temperature (T_i), peak temperature (T_p), final curing temperature (T_f) and curing time can be derived, as in Table 1. With the increasing heating rate, the exothermic peak shifts to a higher temperature and the curing time is shortened.

The processing properties of material are crucial to its application, and the processing temperature is an important aspect of processing properties. In order to get proper schedule parameters of MTPES, extrapolation method is often used [17]. Namely, there was a linear relationship between the temperature (T) and heating rate (β), and the best processing temperature could be acquired when $\beta = 0$ °C/min.

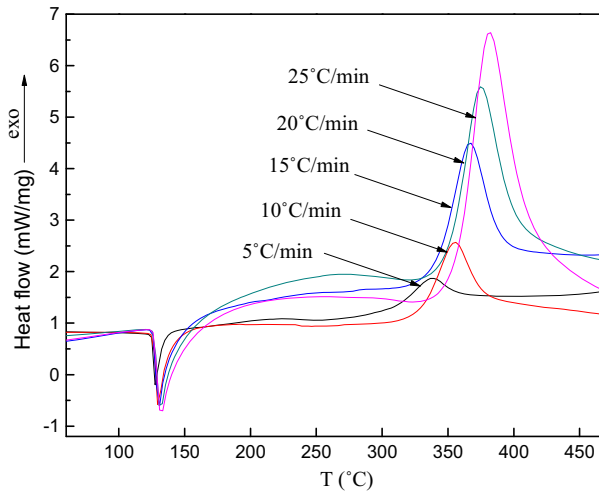


Fig. 2 A typical DSC curves of MTPES at different heating rates

Table 1 Curing parameters of MTPES at different heating rates

β ($^{\circ}\text{C}/\text{min}$)	T_i	T_p	T_f	Curing time (min)	ΔH (kJ/mol)
5	307.4	337.0	366.2	11.76	178.29
10	314.6	356.0	385.4	7.08	131.83
15	320.4	366.0	406.7	5.75	281.16
20	327.7	375.1	413.8	4.31	240.36
25	331.9	381.3	424.5	3.70	232.85

According to the results shown in Fig. 3 and Table 2, the cure schedule of MTPES was determined as follows: (302 $^{\circ}\text{C}$, 1 h) + (331 $^{\circ}\text{C}$, 2 h) + (356 $^{\circ}\text{C}$, 1 h) and the corresponding polymer (PMTPEs) was also obtained by the curing process mentioned above. The typical FT-IR spectra of MTPES and PMTPEs are presented in Fig. 4. The most notable change is that the PMTPEs shows the complete absence of 2168 cm^{-1} ($\text{C}\equiv\text{C}$) and the peak of 1631–1440 cm^{-1} stretching becomes much weaker (aromatic ring), indicating that the cure mechanism might be a radical mechanism leading to a polyene network rather than trimerization of ethynyl group leading to benzene rings, which is consistent with the literature reported [16, 18].

The viscosity–temperature curve of MTPES is shown in Fig. 5. As the temperature increases, the viscosity keeps constant at 80 Pa s and then elevates dramatically at 330 $^{\circ}\text{C}$, corresponding to the gelation temperature of MTPES. Combined with DSC curves and rheological curve, it was shown that the melting point and gelation temperature of MTPES were 130 and 330 $^{\circ}\text{C}$, respectively. This was in agreement with the cure parameters mentioned above, and the 200 $^{\circ}\text{C}$ processing window was able to ensure adequate flow behavior to impregnate other materials for preparing functional composites.

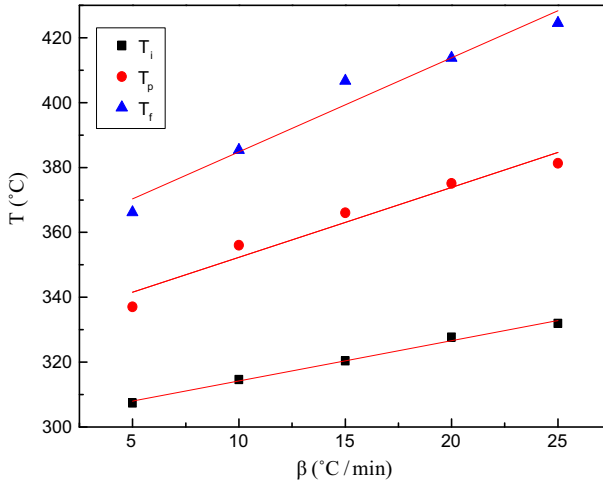


Fig. 3 Linear-fitting plots of cure temperature versus heating rate of MTPES

Table 2 Cure processing parameters of MTPES by linear-fitting method

Temperature	Linear expression	R	Cure parameters ($\beta = 0$ °C/min)
T_i	$Y = 301 + 1.242x$	0.9956	301
T_p	$Y = 330 + 2.154x$	0.9692	330
T_c	$Y = 355 + 2.9x$	0.9733	355

Curing kinetic analysis of MTPES

The accurate time–temperature–conversion curve is of great practical importance for establishing optimum cure parameters. Generally, the kinetic parameters can be calculated using three well-known methods; that is, the Kissinger, Ozawa, and Flynn–Wall–Ozawa methods [19].

The Kissinger method assumes that the maximum reaction rate occurs at the peak temperatures [20]. The equation can be expressed as Eq. (1):

$$\ln \frac{\beta}{T_p^2} = \ln \left(\frac{AR}{E_a} \right) - \frac{E_a}{RT_p} \quad (1)$$

where $\beta = dT/dt$ is the heating rate, t is the time, E_a is the activation energy, R is the universal gas constant, T is the temperature in Kelvin and T_p is the peak temperature. Figure 6 shows the plot of $\ln(\beta/T_p^2)$ against $1/T_p$ for MTPES. The E_a value of 110.38 kJ mol⁻¹ was acquired by Eq. (1).

The Ozawa method assumes that the conversion (α) for different heating rates is constant [21, 22]. The following Eq. (2) can be applied to the thermal data. Thus, the plot of $\ln\beta$ versus $1/T_p$ is a straight line at the same conversion as shown in Fig. 7. The calculated E_a value was 114.90 kJ mol⁻¹

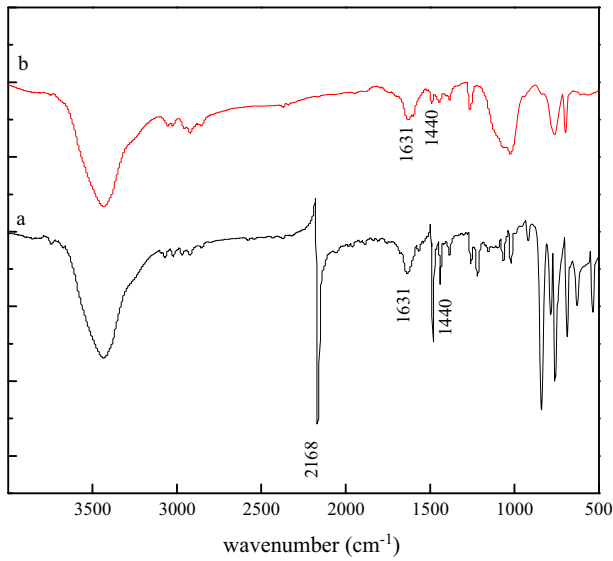


Fig. 4 FT-IR spectra of MTPES (a) and PMTPES (b)

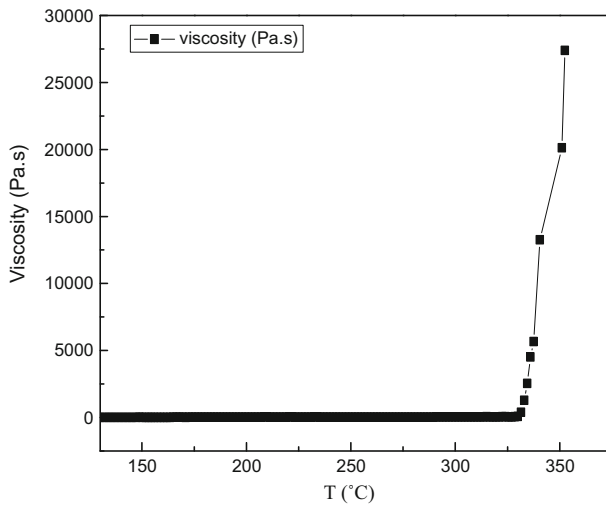


Fig. 5 Viscosity–temperature curve of MTPES

$$\ln \beta = -5.331 - 1.052 \left(\frac{E_a}{RT_p} \right) + \ln \left(\frac{AE_a}{R} \right) - \ln f(\alpha) \quad (2)$$

The Flynn–Wall–Ozawa method [23] is a model-free iso-conversional method, which assumes that both the activation energy and pre-exponential factor are functions of the degree of cure based on Eqs. (3) and (4):

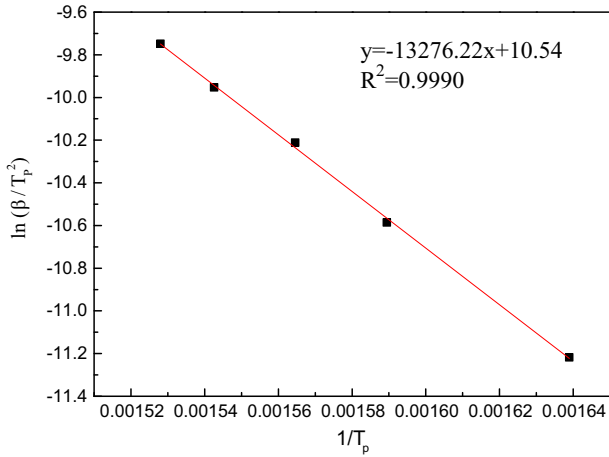


Fig. 6 $\ln(\beta/T_p^2)$ versus $1/T_p$ of MTPES

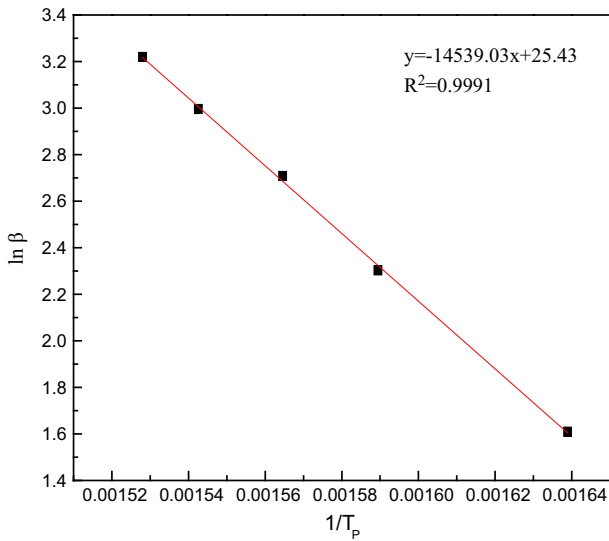


Fig. 7 $\ln \beta$ versus $1/T_p$ of MTPES

$$\ln \beta = \ln\left(\frac{AE_a}{R}\right) - \ln g(\alpha) - 1.052\left(\frac{E_a}{RT}\right) - 5.331 \quad (3)$$

$$g(\alpha) = \int_0^\alpha \frac{d\alpha}{f(\alpha)} \quad (4)$$

Figure 8 shows the temperature versus conversion at different heating rates, and the corresponding curing parameters are also listed in Table 1. As can be seen, with

the increasing of heating rate, the reaction time varies from 3.70 to 11.76 min, indicating that MTPES has a high reactivity. At the same time, the $\ln\beta$ versus $1/T$ is also established in Fig. 9, and the corresponding activation energy is tabulated in Table 3. The average E_a (112.45 kJ/mol) is very close to the results obtained from the Kissinger and Ozawa methods, which further verified that acetylene bond can be initiated in low enthalpy by radical thermal polymerization. As described in the literature [24], the theoretically predicted enthalpy is 189 ± 10 kJ/mol for trimerization based on bond energy calculations, while the experimentally calculated enthalpy is less than the theoretical value, indicating that trimerization is not the major reaction pathway during polymerization. The most probably polymerization is a branched polyene, which could then undergo lots of additional reactions and finally a cross-linked polymer produced [18].

Curing kinetic model analysis of MTPES

In general, the curing mechanism of thermoset is classified into an n th-order reaction and an autocatalytic reaction [25]. The Friedman method [26] is used usually to find proper curing mechanism based on Eq. (5):

$$\ln[Af(\alpha)] = \ln\beta \frac{d\alpha}{dT} + \frac{E_a}{RT} = \ln A + n \ln(1 - \alpha) \tag{5}$$

Therefore, the reaction order n can be obtained from the slope, since the plot of $\ln[Af(\alpha)]$ and $\ln(1 - \alpha)$ yields a straight line for the n th-order reaction. Otherwise, for autocatalytic reaction, the Friedman plot would have a maximum when the $\ln(1 - \alpha)$ is about -0.51 to -0.22 , corresponding to *conversion* at about 0.2–0.4.

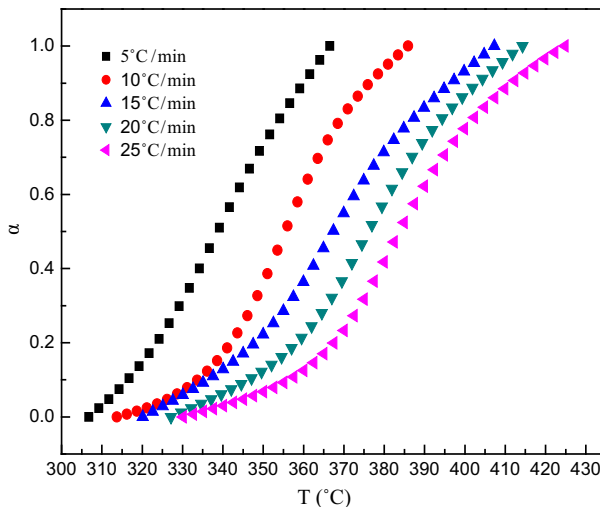


Fig. 8 T versus α of MTPES at different heating rates

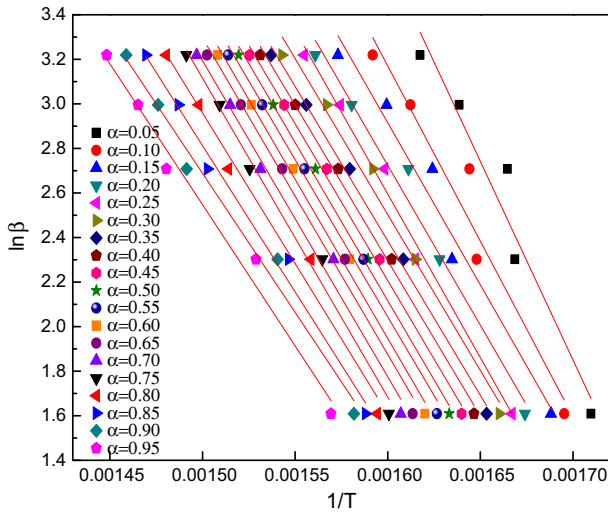


Fig. 9 $1/T$ versus $\ln\beta$ of MTPES at different conversions

Table 3 The parameters obtained from Flynn–Wall–Ozawa method

α (%)	E_x (kJ/mol)	R	α (%)	E_x (kJ/mol)	R
5	140.96	0.9662	55	111.67	0.9952
10	124.46	0.9677	60	113.05	0.9962
15	115.00	0.9808	65	112.36	0.9927
20	113.49	0.9883	70	112.29	0.9921
25	116.22	0.9937	75	113.16	0.9921
30	110.62	0.9921	80	106.87	0.9885
35	109.58	0.9977	85	103.84	0.9928
40	110.46	0.9977	90	98.69	0.9893
45	111.33	0.9977	95	100.19	0.9893
50	112.21	0.9977	Mean	112.45	

This is due to the autocatalytic nature that shows the maximum reaction rate at 20–40 % conversion [27].

Figure 10 depicts Friedman plots of MTPES at different heating rates. Since the plots of $\ln[Af(\alpha)]$ and $\ln(1 - \alpha)$ is not linearly related and evidently shows a maximum in the range of conversion mentioned above, which suggested that the curing reaction is autocatalytic in nature. The autocatalytic nature of MTPES can be explained by the generation of free radical of superoxide or hydrogen peroxide, which is formed by oxygen under at high temperature and these groups accelerate further cleavage of triple bonds to form conjugated a polyene structure [1, 28].

Owing to the autocatalytic characteristics of the MTPES, the reaction can be described by Eqs. (6) and (7):

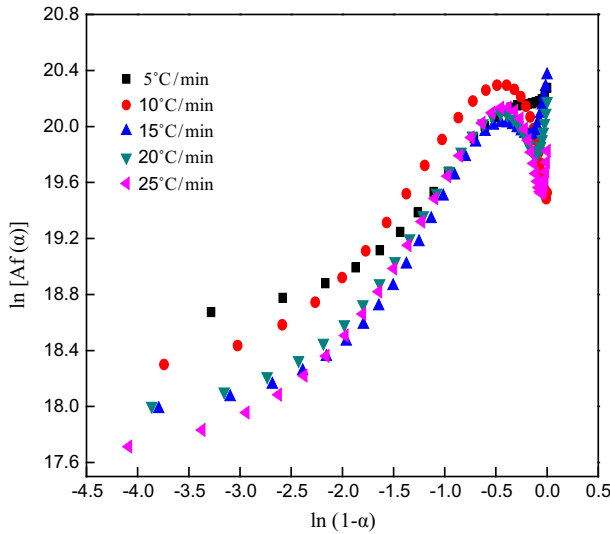


Fig. 10 $\ln[Af(\alpha)]$ versus $\ln(1 - \alpha)$ of MTPES at different heating rates

$$f(\alpha) = (1 - \alpha)^n \alpha^m \tag{6}$$

$$\frac{d\alpha}{dT} = \frac{A}{\beta} \exp\left(-\frac{E_a}{RT}\right) (1 - \alpha)^n \alpha^m \tag{7}$$

then

$$\ln\left(\beta \frac{d\alpha}{dT}\right) + \frac{E_a}{RT} = n \ln(1 - \alpha) + m \ln \alpha + \ln A \tag{8}$$

where m and n are the reaction orders and m describes the autocatalytic characteristics directly. Equation (8) can be solved by multiple linear regression and the values of A , m , and n can be obtained using the average activation energy from different calculated methods, and a is chosen between the beginning of the reaction and the maximum peak of degree of curing ($\alpha = 0.1-0.5$). As a result, the

Table 4 The kinetic parameters evaluated for the curing MTPES

β (°C/min)	E_a (kJ/mol)	$\ln A$ (s ⁻¹)	Mean	n	Mean	m	Mean
5	$E = 112.58$	20.60	21.22	0.79	1.20	0.16	0.56
10		21.41		1.13		0.61	
15		21.26		1.32		0.61	
20		21.01		0.96		0.51	
25		21.83		1.78		0.89	

corresponding result analyses are listed in Table 4. The kinetic mode of MTPES can be described as follows:

$$\frac{dx}{dt} = e^{21.22} \exp\left(-\frac{112580}{RT}\right) (1-x)^{1.20} x^{0.56}$$

Conclusions

Methyl-tri(phenylethynyl)silane (MTPES) was synthesized by Grignard reaction. The curing schedule of MTPES can be determined as follows: (302 °C, 1 h) + (331 °C, 2 h) + (356 °C, 1 h). According to the Kissinger, Ozawa, Flynn–Wall–Ozawa and Friedman methods, the reaction activation energy and the reaction order n , m were 112.58 kJ/mol, 1.20 and 0.56 respectively. The autocatalytic kinetic model was found to be the best description of the curing reaction.

Acknowledgments We gratefully acknowledged the financial support of the National Nature Science Foundation of China (Nos. 51477002, 51303005), the Educational Commission of Anhui Province of China (Nos. KJ2013A087 and KJ2013A095) and the Doctor Foundation of the Anhui University of Science and Technology.

References

1. S.B. Sastri, J.P. Armistead, T.M. Keller, Cure kinetics of a multisubstituted acetylenic monomer. *Polymer* **36**(7), 1449–1454 (1995)
2. M. Itoh, K. Inoue, K. Iwata et al., New highly heat-resistant polymers containing silicon: poly(silyleneethynylene-phenyleneethynylene)s. *Macromolecules* **30**(4), 694–701 (1997)
3. Z. Jiang, Y. Zhou, L. Du, Characterization of a modified silicon-containing arylacetylene resin with POSS functionality. *Chin. J. Polym. Sci.* **29**(6), 726–731 (2011)
4. Y. Wu, R. Yu, L. Hu et al., Thermal stability of cocured blends of vinyl trimethoxysilane and aryl acetylene resins with different posttreatments. *J. Appl. Polym. Sci.* **131**(8), 40158–40163 (2014)
5. S. Tannenbaum, S. Kaye, G.F. Lewenz, Synthesis and properties of some alkylsilanes. *J. Am. Chem. Soc.* **75**(15), 3753–3757 (1953)
6. A.P. Melissaris, M.H. Litt, New high-Tg, heat-resistant, cross-linked polymers. 1. Synthesis and characterization of di-p-ethynyl-substituted benzyl phenyl ether monomers. *Macromolecules* **27**(4), 883–887 (1994)
7. Z.L. Dai, Q. Chen, L.Z. Ni et al., Curing kinetics and structural changes of a di[(N-m-acetylphenyl) phthalimide] ether/[(methyl) diphenylacetylene]silane copolymer. *J. Appl. Polym. Sci.* **100**, 2126–2130 (2006)
8. B. Wrackmeyer, E. Khan, S. Bayer et al., Alkynylsilanes and alkynyl (vinyl) silanes. Synthesis, molecular structures and multinuclear magnetic resonance study. *Zeitschrift für Naturforschung B* **65**(6), 725–744 (2010)
9. I. Kownacki, B. Orwat, B. Marciniec et al., A new and efficient route for the synthesis of alkynyl functionalized silicon derivatives. *Tetrahedron Lett.* **55**(2), 548–550 (2014)
10. C. Hamdouchi, H.M. Walborsky, *Mechanism of Grignard Reagent Formation* (Marcel Dekker, New York, 1996), pp. 145–218
11. Q. Chen, Y. Li, Z.L. Dai et al., Synthesis and characterization of methyl-di (phenylethynyl) silane and its network polymer. *Acta. Chim. Sin.* **63**(3), 254–258 (2005)
12. A. Boudin, G. Cerveau, C. Chuit et al., Reactivity of anionic pentacoordinated silicon complexes towards nucleophiles. *Angew. Chem. Int. Ed.* **25**(5), 473–474 (1986)
13. R. J. Corriu, G. E. Cerveau, C. G. Chuit, et al. Crosslinking agents; drugs. U. S. Pat. 4617413, 1986

14. C. Kim, K. Jeong, I. Jung, Progress toward limiting generation of dendritic ethynylsilanes ($\text{PhC}\equiv\text{C}$)_{4-n}Me_nSi_(n=0-2). *J. Polym. Sci. Part A Polym. Chem.* **38**(15), 2749–2759 (2000)
15. Q. Zhou, X. Feng, L. Ni et al., Novel heat resistant methyl-tri(phenylethynyl) silane resin: synthesis, characterization and thermal properties. *J. Appl. Polym. Sci.* **102**(3), 2488–2492 (2006)
16. Q. Zhou, X. Feng, H.Q. Zhao et al., Curing behavior and thermal property of methyl-tri(phenylethynyl)silane resin. *J. Funct. Polym.* **20**(1), 97–103 (2007)
17. Z. Luo, L. Wei, F. Liu et al., Study on thermal cure and heat-resistant properties of *N*-(3-acetylenophenyl) maleimide monomer. *Eur. Polym. J.* **43**(8), 3461–3470 (2007)
18. Q. Zhou, L. Ni, Thermal cure behavior and pyrolysis of methyl-tri(phenylethynyl) silane resin. *J. Appl. Polym. Sci.* **113**(1), 10–16 (2009)
19. D. Tan, T. Shi, Z. Li, Synthesis, characterization, and non-isothermal curing kinetics of two silicon-containing arylacetylenic monomers. *Res. Chem. Intermed.* **37**(8), 831–845 (2011)
20. H.E. Kissinger, Reaction kinetics in differential thermal analysis. *Anal. Chem.* **29**(11), 1702–1706 (1957)
21. T. Ozawa, Non-isothermal kinetics and generalized time. *Thermochim. Acta* **100**(1), 109–118 (1986)
22. Y. Lu, M. Li, Y. Zhang et al., Synthesis and curing kinetics of benzoxazine containing fluorene and furan groups. *Thermochim. Acta* **515**(1), 32–37 (2011)
23. N. Sbirrazzuoli, Y. Girault, L. Elégant, Simulations for evaluation of kinetic methods in differential scanning calorimetry. Part 3: peak maximum evolution methods and isoconversional methods. *Thermochim. Acta* **293**(1), 25–37 (1997)
24. S.B. Sastri, T.M. Keller, M. Kenneth, Studies on cure chemistry of new acetylenic resins. *Macromolecules* **26**(23), 6171–6174 (1993)
25. C. Jubsilp, K. Punson, T. Takeichi et al., Curing kinetics of benzoxazine-epoxy copolymer investigated by non-isothermal differential scanning calorimetry. *Polym. Degrad. Stab.* **95**(6), 918–924 (2010)
26. H.L. Friedman, Kinetics of thermal degradation of char-forming plastics from thermogravimetry. *J. Polym. Sci. Part C Polym. Symp.* **6**(1), 183–195 (1964)
27. L. Ke, D. Hu, Y. Lu et al., Copolymerization of maleimide-based benzoxazine with styrene and the curing kinetics of the resultant copolymer. *Polym. Degrad. Stab.* **97**(2), 132–138 (2012)
28. A.J. Bissette, S.P. Fletcher, Mechanisms of autocatalysis. *Angew. Chem. Int. Ed.* **52**(49), 12800–12826 (2013)